New Insights into Structural Development in Natural Rubber during Uniaxial Deformation by In Situ Synchrotron X-ray Diffraction

Shigeyuki Toki,* Igors Sics, Shaofeng Ran, Lizui Liu, and Benjamin S. Hsiao*

Department of Chemistry, State University of New York at Stony Brook, Stony Brook, New York 11794-3400

Syozo Murakami, Kazunobu Senoo, and Shinzo Kohjiya

Institute for Chemical Research, Kyoto University, Uji, Kyoto-fu 611-0011, Japan

Received April 15, 2002; Revised Manuscript Received June 7, 2002

ABSTRACT: Molecular orientation and strain-induced crystallization of vulcanized natural rubber during uniaxial deformation were studied via in situ synchrotron wide-angle X-ray diffraction (WAXD). The high intensity of synchrotron X-rays and new image analysis methods made it possible to estimate mass fractions of the strain-induced crystals and the amorphous chains in both oriented and unoriented states. Contrary to the conventional conception, it was found that, in highly stretched natural rubber, most chains remained unoriented in the amorphous phase; only a few percent of the amorphous chains were oriented and the rest of the chains were in the crystalline phase. This indicates that stress induces a network of microfibrillar crystals that is responsible for the elastic properties. The new information has prompted us to reconsider the relationships of molecular orientation, induced crystallization and mechanical behavior in natural rubber.

Introduction

Vulcanized natural rubber under deformation has been the subject of intensive research interest since the 1940s. Several major topics in polymer science such as rubber elasticity theory and structure−property relationships in polymeric solids were initiated from this subject.[1−3] The roles of molecular orientation and deformation-induced crystallization were found to be of particular importance because of their effect on the final mechanical properties.[2,4] However, despite the enormous knowledge base developed thus far, some interesting "new" insights into this "old" subject have been obtained in the current study, which is the purpose of this article.

Many in situ deformation studies of natural rubber have been carried out in the past.[3−16] For example, in situ birefringence measurements have been demonstrated to be useful for characterizations of total molecular orientation of crystalline and amorphous phases.[3−11] Treloar first reported that birefringence increased with strain as well as with stress.[3] The relationship between stress and birefringence was almost constant at a fixed strain (thus a constant stress-optical coefficient), which has become a critical justification for the rubber elasticity theory. Stein and coworkers[5,6] used birefringence data to deduce the increase of crystallinity during isothermal crystallization at a fixed strain. Toki et al.[10,11] demonstrated that birefringence increased linearly with strain and suggested that affine deformation might be applicable even at large strains under a practical rate of deformation. The studies with in situ X-ray diffraction techniques[14−16] have also been demonstrated. Shimomura et al.[15] and Toki et al.[16] showed that crystallinity increased with strain. Mitchell[17] concluded that strain-induced crystallization started around 400% of strain and the maximum achievable crystallinity was around 30% with a conventional WAXD analysis. He suggested some possible modifications to the affine model used in the rubber elasticity theory.

It is clear that on the basis of the existing concept of rubber elasticity, one frequently ignores the nature of amorphous chains—all amorphous molecules are assumed to be oriented with strain, whereas crystallization occurs sporadically. However, our current results, obtained from the U.S. and Japanese teams independently, painted a slightly different picture. It was found that, during the stretching of natural rubber, only a small fraction of the amorphous chains are oriented and they are subsequently crystallized during stretching, carrying most of the applied load, while the majority of amorphous chains remain unstretched. The current studies were conducted using an in situ synchrotron wide-angle X-ray diffraction (WAXD) technique to monitor the changes in the local molecular structure during deformation. The high intensity of synchrotron X-rays offered a major advantage over the conventional in-laboratory X-ray method, which restricted the measurement to being carried out in a stretch-hold mode. (During WAXD measurement using an in-laboratory source, one must stop stretching and hold the deformation of the sample.) When the stretching was stopped, stress was relaxed and microstructures often changed, which significantly altered the state of interest. In this paper, the use of synchrotron X-rays enabled both Japanese and U.S. teams to observe the dynamic crystallization behavior of natural rubber in real time. The Japanese team recently reported a part of this work elsewhere.[18] New results using a novel image analysis method will be presented here.

Experimental Section

Synchrotron measurements were carried out at the X27C beam-line in the National Synchrotron Light Source (NSLS),

* To whom correspondence should be addressed. E-mails: stoki@mail.chem.sunysb.edu; bhsiao@notes.cc.sunysb.edu.

10.1021/ma0205921 CCC: $22.00
Published on Web 07/20/2002

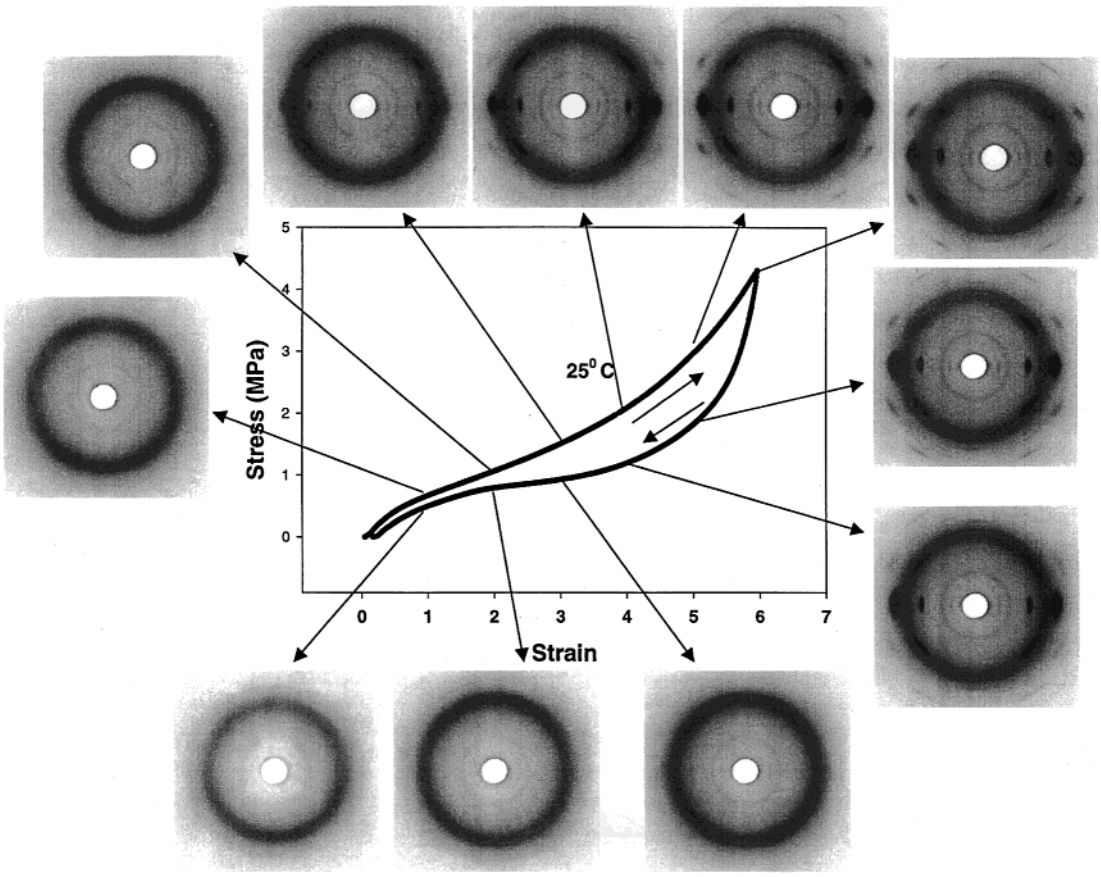

Figure 1. Stress−strain relationship and selected WAXD patterns collected during stretching and relaxation of natural rubber (results from the U.S. team). Each image was taken at the strain indicated by the arrows.

Brookhaven National Laboratory (BNL), NY, and at the BL40XU beam-line in the Japan Synchrotron Radiation Research Institute (JASRI), SPring-8, Hyogo, Japan, independently. The wavelengths used in X27C and in BL40XU were 1.307 and 1.00 Å, respectively. The two-dimensional WAXD patterns were recorded by a Bruker Smart 1500 X-ray detector for quantitative image analysis at X27C, NSLS, and by a CCD camera (Hamamatsu C4880) at BL40XU of JASRI. The typical image acquisition times for both experiments were 10 s in Japan and 30 s in the United States. All the measured WAXD images were corrected for beam fluctuation and sample absorption.

Both tensile machines used in the United States and in Japan allowed symmetric deformation of the sample, which permitted the focused X-ray to illuminate the same sample position during stretching. The chosen deformation rate was 10 mm/min for both studies. The experiments were carried out at room temperature. The U.S. instrument was developed by a modification of a tabletop stretching machine from Instron, Inc. The Japanese machine has been developed independently and described in detail elsewhere.[19,20]

Both research teams have studied sulfur-vulcanized natural rubber samples with only a very slight difference. The recipes and cure conditions for preparation of the samples are listed in Table 1. The chosen recipe was for typical vulcanized natural rubber similar to that of Treloar's classic compound.[3] The apparent values of the degree of cross-linking, characterized by the number ν of moles of cross-links per cubic meter, were estimated from the tensile elastic modulus using the simple molecular theory of rubber elasticity.[2] The value ν was 1.8×10^2 mol/m^3 ; the average molecular weight between network points was around 5000 g/mol, if the cross-links were distributed homogeneously.

Table 1. Recipe and Cure Condition for Preparation of the Rubber Samples[a]

NR	100
stearic acid	2.0
antioxidant	1.0 (MBMTB)
active ZnO	1.0
accelerator	1.0 (TBBS)
sulfur	1.5

[a] NR: U.S. sample: SMR-L: standard Malaysian rubber, light color. Japan sample: SMR-5: standard Malaysian rubber number 5. Cure condition: U.S.: 160 °C for 60 min; Japan: 145 °C for 60 min.

Results and Discussion

The stress−strain relation and selected WAXD patterns (collected at X10A, NSLS) during stretching and retraction are shown in Figure 1. All images were normalized with respect to the sample thickness change, sample absorption, and beam fluctuation. The arrow indicates the average strain value where the image was taken. The high intensity of synchrotron X-rays makes it possible to collect the WAXD patterns during deformation in real time without holding. In Figure 1, it is seen that highly oriented crystalline reflection peaks begin to appear at strain around 3.0. The intensities of these reflections increase with strain during stretching and decrease upon retraction. The stress−strain curve shows a hysteresis, typically found in pure vulcanized natural rubber. This hysteresis corresponds well with the different appearance in the WAXD images collected at the same strain during stretching and retraction. In Figure 1, it is interesting to note that an intense amorphous halo remains very much intact in WAXD during both processes of stretching and retraction. This feature in WAXD has never been fully analyzed before.

The behavior of strain-induced crystallization and the persistence of the amorphous phase can be identified by the linear diffraction profiles taken along the equator

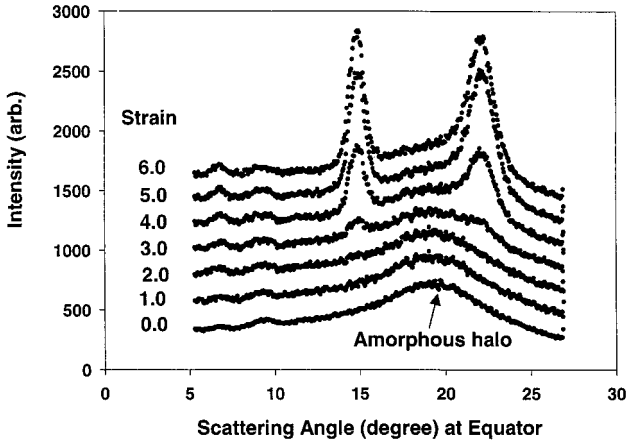

Figure 2. Equatorial diffraction profiles taken from Figure 1 as a function of strain under stretching.

from the two-dimensional WAXD images collected at different strains during stretching (Figure 2). Two distinct crystal diffraction peaks, which can be indexed as the 200 and 120 reflections, first appear at strain = 3.0. Although the intensities of the two diffraction peaks increase with strain, the peak intensity of the amorphous halo ($2\theta \approx 20°$) only decreases slightly during deformation, indicating the persistence of sizable amorphous chains in the highly stretched sample.

The above behavior has also been observed in a similar natural rubber studied by the Japanese team. Figure 3 illustrates WAXD images (collected at BL40XU, JASRI) of the sample prior to stretching (the initial state, Figure 3a) and during stretching at the strain of 5 (Figure 3b). It is seen that before stretching, this natural rubber exhibits a halo pattern in WAXD, indicating that all chains are amorphous with no preferred orientation. At strain = 5 (Figure 3b), the WAXD pattern exhibits ordered crystal reflections, indicating the occurrence of strain-induced crystallization. The induced crystal structure is consistent with a monoclinic unit cell with parameters $a = 1.25$ nm, $b = 0.89$ nm, c (chain axis) $= 0.81$ nm, and $\beta = 92°$, which has been reported by Bunn.[21] The persistence of large fractions of amorphous chains can also be verified by the following analysis. The intensity at the peak position of the amorphous halo along the meridian and equatorial directions have been determined as I_a(m) and I_a(e), respectively, in the stretched sample (Figure 3c). I_a(e) consists of contributions from both oriented and unoriented amorphous chains. In contrast, I_a(m) consists of contribution from only unoriented amorphous chains. It is found that I_a(e) is larger than I_a(m) by only about 5%, which suggests that the majority of the amorphous chains are isotropy without preferred orientation during stretching. The nature of the crystalline phase induced by deformation is seen in Figure 3d. The observed reflection peaks can be indexed by the monoclinic unit cell (Figure 3d). The azimuthal spread of the strong equatorial (120) crystalline reflection has also been estimated (Figure 3d), which is found to be very narrow. This result suggests that the induced crystallites are well-oriented along the stretching direction. The fraction of unoriented crystallites is negligible because no circle patterns can be observed except for the amorphous halo. Results of this analysis have already been reported elsewhere.[18]

The quantitative evaluation of mass fractions of the crystal and amorphous (oriented and unoriented) phases can be determined with a novel two-dimensional image analysis method developed by the U.S. group.[22] The procedures for the analysis are illustrated in Figure 4. The WAXD pattern taken from the unstretched sample is shown in Figure 4a, which exhibits an isotropic amorphous halo with no preferred orientation. At strain = 6, the WAXD pattern (Figure 4b, the data from Figure 1) shows the superposition of the oriented strain-induced crystalline diffraction pattern and the isotropic residual amorphous halo. The isotropic and anisotropic contributions in Figure 4b have been deconvoluted using a two-dimensional analytical method, which is briefly described here. The isotropic fraction of the scattered intensity was obtained by connecting the minimum values of the scattered intensity on the azimuthal scans taken at different scattering angles. The envelope of these minimum values was smoothed and fitted with two-dimensional functions (e.g., Gaussian). The deconvolution procedures were described elsewhere.[22] The two-dimensional isotropic contribution extracted from the WAXD pattern at strain = 6 is illustrated in Figure 4c, which exhibits near identical features to the original WAXD pattern prior to stretching (Figure 4a). The deconvoluted anisotropic contribution of the WAXD pattern is shown in Figure 4d, which is composed of oriented crystalline reflection peaks and a very small amount of oriented amorphous phase conjugated on the equator between the strong 120 and 200 diffraction peaks. A two-dimensional (2D) peak fit routine was then used to fit all the crystal diffraction peaks and the oriented amorphous peak (centered on the equator). The fitted intensity profile of the 120 and 200 reflection peaks and the oriented amorphous peak on a half diffraction pattern around the equator is shown in Figure 4e. The mass fraction of the strain-induced crystal can be estimated by dividing the sum of the crystal diffraction intensity by the total scattered intensity, which is about 20% for strain = 6; the corresponding mass fraction of the oriented amorphous phase is only about 5% (near the detection limit). We note that the estimated crystal fraction may be slightly lower than the true value as some meridianal reflection peaks cannot be intercepted by the diffraction sphere.

The changes of mass fractions of the strain-induced crystals and the oriented amorphous phase during stretching and retraction are shown in Figure 5. During stretching, the mass fraction of the total anisotropic scattering is estimated to be about 7% at strain = 2. No crystal reflection peaks can be identified at this stage; the anisotropic scattering is thus due to the oriented amorphous chains. It appears that crystallization begins at strain = 2.5, where the fraction of the oriented amorphous chains starts to decrease and the fraction of the induced crystals starts to increase. At strain = 3.0, the fractions of the crystalline phase and the oriented amorphous phase are almost identical. At strain larger than 3, the crystalline phase becomes dominant, where the fraction of the oriented amorphous phase remains between 4 and 5%. From the above observation, we can conclude that the oriented amorphous chains are precursors to the induced crystals. The phenomena seem to be similar to the stress-induced crystallization during fiber spinning.[23] The crystallization rate from the oriented chains must be very fast, probably in the order of 60 m/s, as reported by Mitchell et al.[24] In addition, it is reasonable to rationalize that

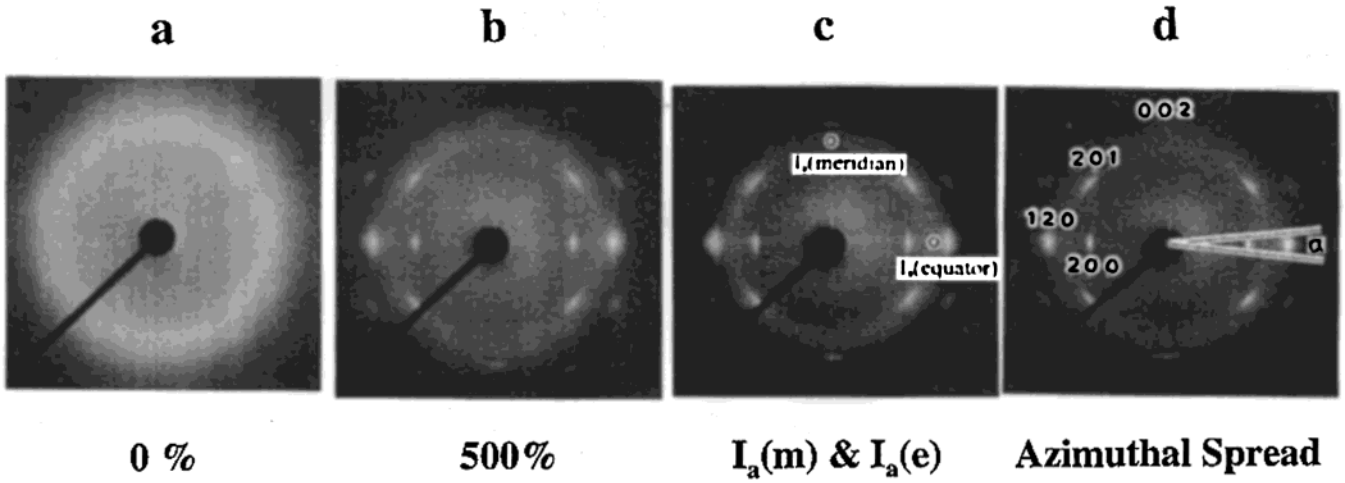

Figure 3. Selected WAXD patterns collected during deformation of natural rubber (results from the Japanese team): (a) before stretching; (b) during stretching at strain = 5; (c) analysis of amorphous intensities $I_a(e)$ and $I_a(m)$; (d) the analysis of azimuthal spread on the crystal 120 reflection peak. The crystal reflection peaks can be indexed by a monoclinic cell with unit cell parameters of $a = 1.25$ nm, $b = 0.89$ nm, $c = 0.81$ nm, and $\alpha = 92°$.[25]

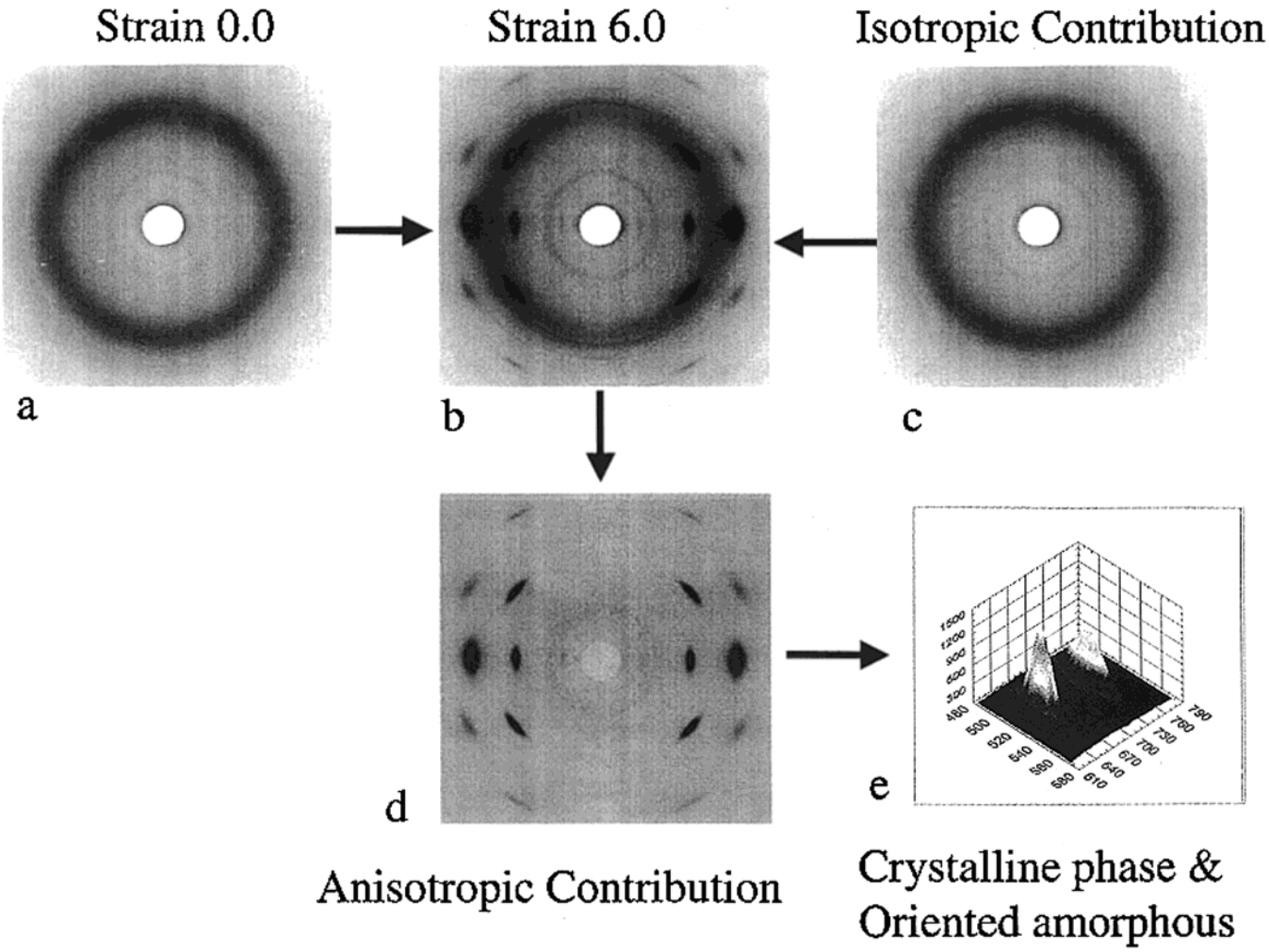

Figure 4. Raw WAXD patterns collected during deformation of natural rubber (results from the U.S. team): (a) before stretching; (b) during stretching at strain = 6; (c) extracted isotropic contribution or the unoriented amorphous phase (the intensity was not normalized); (d) extracted anisotropic contribution (sum of the crystal and oriented amorphous phases); (e) extracted oriented amorphous contribution and crystalline peaks. (Scales are plotted in pixels. The crystal reflection (200) is around 640 pixels and the reflection (120) is around 730 pixels. The oriented amorphous peak is small and around 700 pixels.)

the strain-induced crystallites are in the extended chain crystal form having a microfibrillar structure. As only a small fraction of chains are oriented and crystallized (20%), this suggests that the strain-induced crystallites form an additional physical cross-linking network, carrying most of the applied load.

The above results indicate that even under a very high deformation state (e.g., strain = 6), the majority

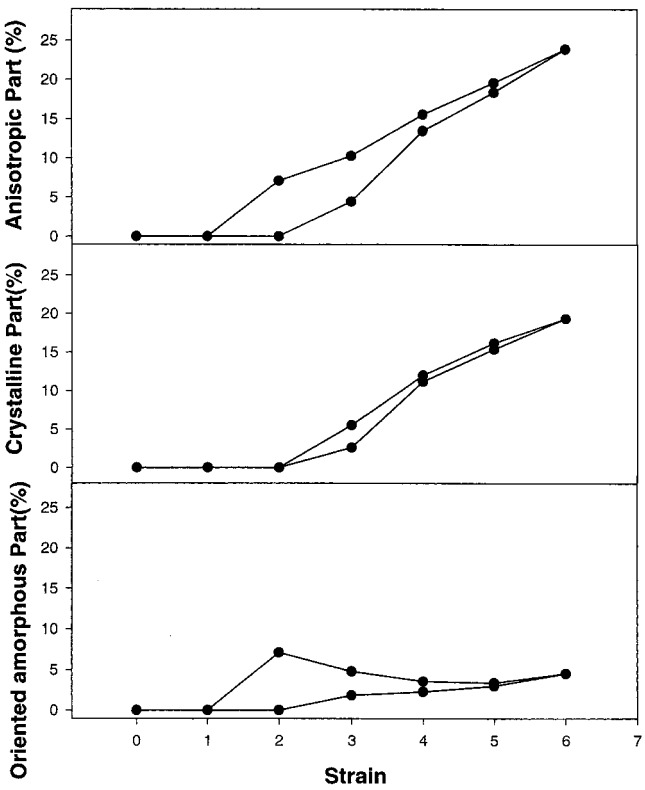

Figure 5. Anisotropic fractions (the total fraction, fractions of crystalline phase and oriented amorphous phase) at each strain during stretching and relaxation.

of the chains remain unoriented (75%). This behavior seems to be very universal in rubbery materials, but it has never been fully analyzed before. For example, Gehman and Field,[25] Luch and Yeh,[26] and Shimomura et al.[15] reported similar WAXD images containing a noticeable unoriented amorphous pattern superimposed on the crystalline reflections under deformation. Although these classic WAXD images were taken with a conventional X-ray source and the stretch−hold method, they showed clear evidence of an amorphous halo. Therefore, our observed patterns are not new but the quantitative analysis that a large fraction of unoriented phase exists at large strains during stretching is new.

To further evaluate the validity of our results, we have used the published birefringence data obtained from stretching of rubber samples having similar compositions for the following exercise. Hashiyama et al.[6] has proposed a simple relationship between the total birefringence (Δn) and the crystallinity (ϕ_c) for rubber as follows,

$$\Delta n = \phi_C \Delta n_C + (1 - \phi_C)\Delta n_A + \Delta n_F \qquad (1)$$

where Δn_C and Δn_A represent the birefringence of the crystalline and amorphous phases, respectively, and Δn_F is the form of birefringence arising from the interphase between the crystalline and amorphous phases. During deformation, the stretched sample can be considered as having four different states of polymer chains.

total molecules at the deformed state =
ϕ_{OA} (oriented amorphous phase) +
ϕ_{OC} (oriented crystalline phase) +
ϕ_{UA} (unoriented amorphous phase) +
ϕ_{UC} (unoriented crystalline phase) (2)

Our results indicate that ϕ_{UC} is negligible but ϕ_{UA} is relatively large. Because the fractions of the oriented amorphous phase ϕ_{OA} and the oriented crystallites ϕ_{OC} are responsible for the birefringence changes, whereas the unoriented amorphous phase ϕ_{UA} and the unoriented crystalline phase ϕ_{UC} are not, we can modify eq 1 as

$$\Delta n = \phi_{OC}\Delta n_C + \phi_{OA}\Delta n_A + \Delta n_F \qquad (3)$$

The difference between the values $(1 - \phi_C)$ and (ϕ_{OA}) is very large because the value ϕ_{UA} is not negligible (note $\phi_A = \phi_{UA} + \phi_{OA}$). Birefringence of the crystalline phase can be calculated as follows,[6,15]

$$\Delta n_C = f_C \Delta n_{CI} \qquad (4)$$

where f_C is the crystal orientation function and Δn_{CI} is the intrinsic birefringence of the crystalline phase. The last two variables are known for the tested rubber: f_C is about 0.93, which has been calculated from Figure 2,[18] and the intrinsic birefringence of the crystalline phase is 0.130.[6] The birefringence of the oriented amorphous phase can also be estimated using the following method,

$$\Delta n_A = f_A \Delta n_{AI} \qquad (5)$$

where f_A represents the orientation function of the amorphous phase and Δn_{AI} represents the intrinsic birefringence of the amorphous phase. Although the value of f_A depends on the deformation strain, f_A may be assumed to be unity at high strain. The intrinsic birefringence of the amorphous phase of polyisoprene has been reported before, which is 0.2 ± 0.02.[17] The birefringence of natural rubber at high strain thus can be estimated as $0.034 \pm 0.001 + \Delta n_f$. This estimate is somewhat consistent with the low experimental birefringence data measured during deformation of natural rubber. For example, the following birefringence data have been published: 0.005 at strain = 3.0,[15] 0.015 at strain = 6.0,[10] 0.018 at strain = 4.0,[2] 0.025 at strain = 4.0,[6] and 0.035 at strain = 4.0.[27] Although these small values of birefringence of natural rubber during deformation have been considered as a contribution of the low degree of orientation of deformed molecules, our results have indicated otherwise. Our study suggests that the small value of measured birefringence is caused by the small fraction of highly oriented molecules. In other words, we conclude that the birefringence in natural rubber is a direct measure of the degree of crystallinity because the oriented amorphous phase is quite small.

It appears that the strain-induced crystallization does not affect the stress−strain relationship directly. This is because the increase of the crystalline phase is almost linear (Figure 5) but the increase of stress has an S-shape (Figure 1). Several researchers[2,9,10,16] have pointed out that the upturn of stress did not infer the start of crystallization; our results concur with their findings. However, we still noted a large difference in stress at high strain between the stretching and retraction processes, which is caused by strain-induced crystallization.[2,16,25] We argue that, during stretching, the initial stress is mainly determined by vulcanized chains in the cross-linking network, whereas the final stress is determined by the network of strain-induced crystallites. During retraction, as some induced crystallites do

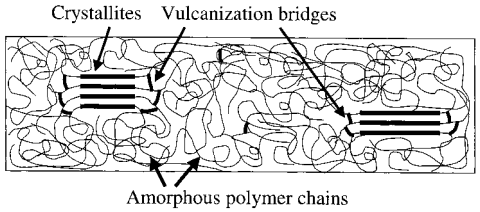

Figure 6. Schematic diagram of vulcanized rubber deformed at large strains (A, crystallites; B, vulcanized network (sulfur bridge); C, amorphous polymer chains).

not melt immediately, the effective network structure becomes different from the structure induced directly by stretching. This forms the base for the hysteresis loss in stress.

Finally, we have illustrated the schematic diagram of deformed network chains in natural rubber under larger strain in Figure 6. This diagram was constructed based on some prior knowledge of natural rubber, which can be summarized as follows.

1. The network points in natural rubber are not distributed homogeneously because the vulcanization process is essentially a chemical reaction taken place in the pseudo-solid state. Once the chemical reaction is initiated, connecting two adjacent long-chain molecules, the viscosity in the network vicinity increases significantly, making sulfur molecules extremely difficult to disperse freely. As a result, the vulcanized networks can possess both densely as well as lightly cross-linked domains. In other words, vulcanized natural rubber is not a homogeneous cross-linked material.

2. The network structure in natural rubber does not consist of cross-linking points but short-chain cross-linking bridges between the adjacent molecules (Figure 6). This is because the sulfur molecule has a cyclic structure containing 8 sulfur atoms, S_8, before vulcanization. After vulcanization, the sulfur molecule generates a bridge chain between two adjacent polyisoprene molecules, which may possess chemical compositions of monosulfur $-S-$, disulfur $-S-S-$, and polysulfur $-Sx-$ ($x = 3-8$).[26,27] Although the network bridge may consist of different sulfur atoms, short bald lines are used to represent the bridge chains without distinguishing the chain length in Figure 6.

3. The network bridges (sulfur chains) may have two opposite effects on strain-induced crystallization during different stages of stretching. First, the bridges can enhance molecular orientation of chains in the vicinity of cross-links under deformation, thus induced crystallization of polymer chains. Second, these bridges may also hinder the growth of the crystalline structure. This argument is supported by the pulsed NMR study of stretched rubber samples, which showed that the lower molecular weight chains between cross-linked points facilitated deformation-induced crystallization at the same strain when compared to higher molecular weight chains between cross-linked points.[29] Therefore, crystallization must be initiated in the dense network region having shorter molecular weight chains between the network bridges.

4. The vicinity of the cross-linked chains should bear the majority of the applied stress because the elastic modulus of vulcanized rubber is proportional to the number of network chains. We may consider several known facts here to understand the mechanical behavior of natural rubber under deformation. (1) The theoretical calculation on entropy forces of the non-Gaussian chains between network points has been successfully used to elucidate stress−strain relation of natural rubber with classical Treloar's experimental data (no crystallization was induced).[30] (2) The highly oriented polymer chains tends to crystallize very rapidly,[24] which has also been seen in this study. The dense network regions should become harder by deformation because of the induced crystallites. This behavior has been reported in swollen deformed gel materials with small-angle neutron scattering (SANS).[31,32] These observations suggest that the mechanical behavior of natural rubber should be considered by combined theories of non-Gaussian deformed chains and the dynamic induction of crystallites.

5. Our results showed that about 75% of polymer chains did not exhibit any orientation under large deformation strain. These chains must be in the random coil state that are surrounded by highly oriented chains or induced crystals connected through network bridges. This phenomenon is caused by the inhomogeneity of the network formation during vulcanization.

Conclusions

In situ synchrotron X-ray diffraction study of natural rubber during mechanical deformation revealed that the majority of molecules (up to 75% of the mass) remain in the random-coil state even at large strains. The fraction of the strain-induced crystallites at high strains is about 20%, where the corresponding fraction of the oriented amorphous phase is about 5%. These results inspire us to reconsider the role of orientation and strain induced crystallization in the mechanical properties of natural rubber because most rubber have been considered to contain oriented chains. The oriented amorphous molecules do not increase with strain because these molecules tend to form the crystalline phase quite readily. These results are consistent with the low values of the birefringence data collected at large strain, which appears to be a direct measure for the fraction of induced crystallinity. The unexpected structural changes in natural rubber under deformation are caused by the inhomogeneity of the network formation during vulcanization.

Acknowledgment. The financial support of the U.S. team was provided by the National Science Foundation (DMR- DMR 0098104). The synchrotron beamline X27C at the NSLS was supported by the Department of Energy (Grant DE-FG02-99ER 45760). The Japanese team appreciates Dr. Y. Nishikawa's (Riken Harima Institute) and Mr. K. Inoue's (SPring-8) assistance in the study.

References and Notes

(1) Flory, P. J. *Principles of Polymer Chemistry*; Cornell University Press: Cornell, 1953.
(2) Treloar, R. G. *The Physics of Rubber Elasticity*, 3rd ed.; Oxford University Press: Oxford, 1975.
(3) Treloar, R. G. *Trans. Faraday. Soc.* **1947**, *43*, 277 and 284.
(4) Gent, A. N. *Trans Faraday Soc.* **1954**, *50*, 521.
(5) Stein, R. S. *Rubber Chem. Technol.* **1976**, *49*, 459.
(6) Hashiyama, M.; Gaylord, R.; Stein, R. S. *Makromol. Chem. Suppl.* **1975**, *1*, 579.
(7) Mukherjee, D. P. *Rubber Chem. Technol.* **1974**, *47*, 1234.
(8) Suzuki, A.; Oikawa, H.; Murakami, K. *J. Macromol. Sci. Phys.* **1985**, *B23*, 535.
(9) Choi, I. S.; Roland, C. M. *Rubber Chem. Technol.* **1997**, *70*, 202.
(10) Toki, S.; Sen, T. Z.; Valladares, D.; Cakmak, M. Presented at the ACS Rubber Div. Spring Meeting 2001, paper no. 12.

(11) Toki, S.; Sen, T. Z.; Valladares, D.; Cakmak, M. Presented at the ACS Rubber Div. Fall Meeting 2001, paper no. 42.
(12) Gotoh, R.; Takenaka, T.; Hayama, N. *Kolloid-Zeit. Zeit. Polym.* **1965**, *205*, 1.
(13) Siesler, H. W. *Appl. Spectrosc.* **1985**, *39*, 761.
(14) Oono, R.; Miyasaka, K.; Ishikawa, K. *J. Polym. Sci. Polym. Phys.* **1973**, *11*, 1477.
(15) Shimomura, Y.; White, J. L.; Spruiell, J. E. *J. Appl. Polym. Sci.* **1982**, *27*, 3553.
(16) Toki, S.; Fujimaki, T.; Okuyama, M. *Polymer* **2000**, *41*, 5423.
(17) Mitchell, G. R. *Polymer* **1984**, *25*, 1562.
(18) Murakami, S.; Senoo, K.; Toki, S.; Kohjiya, S. *Polymer* **2002**, *43*, 2117.
(19) Murakami, S.; Tanno, K.; Tsuji, M.; Kohjiya, S. *Bull. Inst. Chem. Res. Kyoto Univ.* **1995**, *72*, 418.
(20) Murakami, S. *J. Chem. Soc. Jpn.* **2000**, *2*, 142.
(21) Bunn, C. W. *Proc. R. Soc. A* **1942**, *180*, 40.
(22) Ran, S.; Fang, D.; Zong, X.; Hsiao, B. S.; Chu, B.; Cunniff, P. M. *Polymer* **2001**, *42*, 1601.
(23) Ziabicki, A.; Jarecki, L. *High-Speed Fiber Spinning: Science and Engineering Aspects*; Ziabicki, A., Kawai, H., Eds.; Wiley: New York, 1985.
(24) Mitchell, J. C.; Meier, D. J. *J. Polym. Sci. A-2* **1968**, *6*, 1689.
(25) Gehman, S. D.; Field, J. E. *J. Appl. Phys.* **1939**, *10*, 564.
(26) Luch, D.; Yeh, G. S. Y. *J. Macromol. Sci. Phys.* **1973**, *B97*, 121.
(27) Coran, A. Y. *Rubber Chem. Technol.* **1964**, *37*, 668.
(28) Nakauchi, H. *J. Soc. Rubber Ind. Jpn.* **2002**, *75*, 73.
(29) Nishi, T.; Chikaraishi, T. *J. Macromol. Sci. Phys.* **1981**, *B19*, 445.
(30) Boyce, C.; Arruda, E. M. *Rubber Chem. Technol.* **2000**, *73*, 504.
(31) Mendes, E., Jr.; Linder, P.; Buzier, M.; Boue, F.; Bastide, J. *Phys. Rev. Lett.* **1991**, *66*, 1595.
(32) Mendes, E.; Oeser, R.; Hayes, C.; Boue, F.; Bastide, J. *Macromolecules* **1996**, *29*, 5574.

MA0205921